
Stormwater runoff plumes observed by SeaWiFS radiometer in the Southern California Bight

*Nikolay P. Nezlin, Paul M. DiGiacomo¹,
Eric D. Stein and Drew Ackerman*

ABSTRACT

Understanding the factors that influence the incidence and dispersal patterns of freshwater runoff plumes in southern California is important for management of coastal water quality. Significant river discharge is associated with episodic winter rainstorms, leading to turbid pollutant and pathogen-laden stormwater plumes that are clearly visible near shore in the Southern California Bight (SCB). We analyzed 1.1-km spatial resolution sea-spectral reflectance data acquired from 1997 to 2003 by the Sea-viewing Wide Field-of-view Sensor (SeaWiFS), focusing on four regions with distinctive adjacent watershed properties: Ventura, Santa Monica Bay, San Pedro Shelf, and Orange County/San Diego. The area of each plume was detected by the backscattering characteristics of surface waters, i.e., normalized water-leaving radiation of green-yellow wavelength 555 nm (nLw555). Plume area size was correlated with rainstorm magnitude, which was estimated from atmospheric precipitation averaged over the total area of the watersheds connected to the seashore. The time lag between rainstorm and maximum plume was one day in San Pedro Shelf region and two days in the other three regions. Assessing maximum correlation between precipitated rainwater and plume size, we estimated the optimal nLw555 values best characterizing plume boundaries in each of the four study regions. Another quantitative characteristic derived from this correlation between rainwater and plume size was defined as the coefficient of persistence, a relationship between the speed of freshwater discharge and the time of plume water dissipation; this coefficient varied according to watershed. The primary factors regulating the relationship between rainstorm and plume area were watershed land-use characteristics, size, and elevation.

INTRODUCTION

Water quality in the Southern California Bight (SCB) is impacted by seasonally variable river

runoff. The runoff is a primary source of contaminants that can negatively impact human and ecosystem health and productivity (Ackerman and Weisberg 2003, Bay *et al.* 2003, Noble *et al.* 2003, Schiff and Bay 2003, Reeves *et al.* 2004). Winter rainstorm events lead to episodic peaks in runoff, often resulting in high near-shore bacterial counts that can force closures of recreational beaches due to associated human health risks (Cabelli *et al.* 1982, Haile *et al.* 1999). Strong rainstorms are especially hazardous, because the concentration of bacteria in stormwater increases with increasing rainstorm intensity (Reeves *et al.* 2004). Intensive stormwater discharge after rainstorms produce plumes that are easily distinguished from ambient marine waters by their high concentration of suspended matter, which changes the color of the ocean surface (Mertes *et al.* 1998, Sathyendranath 2000, Mertes and Warrick 2001). The movement and persistence of plumes may be influenced by a variety of factors, such as wind and ocean circulation, as well as the volume, timing, and intensity of stormwater discharge. Knowledge of the factors influencing and regulating plume dynamics is important to coastal managers, who are responsible for short-term management and long-term policy decisions to protect water quality and human health for the millions of residents who annually use Southern California beaches and coastal waters.

Stormwater plumes are typically studied using data collected from buoys and research vessels. However, such traditional oceanographic methods cannot resolve detailed spatio-temporal patterns of stormwater plume dynamics due to a characteristically limited number of stations (and/or samples) resulting from logistics, cost, weather, or other constraints. This problem can be partly solved by utilizing existing satellite observations of visible spectral radiance (~ocean color), regularly (nominally daily) collected by NASA imaging spectroradiometers in low Earth orbit (e.g., Esaias *et al.* 1998, McClain *et al.* 2004). Cloud cover leading to missing data is common,

¹California Institute of Technology, Jet Propulsion Laboratory, Pasadena, CA

presenting a challenge when using ocean color imagery. However, this situation is somewhat mitigated in Southern California by the high pressure systems that often follow winter storms, which typically serve to clear the skies in this region, and the daily acquisition of ocean color data. Level 2 (1.1-km spatial resolution) data and associated imagery, collected since autumn 1997 from the SeaWiFS, provide an extensive data set for statistical analysis of plume dynamics and investigation of potential controlling factors in different sub-regions of the Southern California coastal zone.

In this study, we analyze discharge-plume dynamics in four regions of the SCB (Figure 1). In a previous study based on SeaWiFS observations, Nezlin and DiGiacomo (2005) analyzed the statistical relationship between the amount of precipitated stormwater and the dynamic characteristics of plumes over the San Pedro Shelf, which is adjacent to a highly urbanized coastal watershed. They estimated that normalized water-leaving radiation at 555 nm (\sim green-yellow band; nLw_{555}) of a level $>1.3 \text{ mW cm}^{-2} \mu\text{m}^{-1} \text{ sr}^{-1}$ appeared to be the best fit for distinguishing runoff plumes from ambient waters. The persistence of plumes was estimated by fitting the coefficients of the model of plume water dissipation (see Equation 1 in Methods) to achieve maximum correlation between the plume area and rainstorm. It remained unclear, however, the extent to which the observed relationships were applicable to other areas of the SCB. Comparing the quantitative relationship between rainstorm and plume size relative to different regions of the Southern California coast, we focus on the differences between the catchment areas (watersheds) where stormwater is precipitated, infiltrated, and discharged to the coastal ocean.

Our goals are:

- To quantify area size of runoff plumes within the SCB using SeaWiFS observations from October 1997 to June 2003, specifically identifying nLw_{555} values that serve as the optimal plume boundary indicator in different regions;
- To explore the correlation between plume area and the amount of stormwater discharged from coastal watersheds in different sub-regions of the SCB, with a focus on the time lag between rainstorms, extent of plume, and persistence of the plume;

- To describe typical sizes and patterns of stormwater plumes in different regions of the SCB; and
- To relate the correlations between rainstorms, plumes, and the physiographic and land-use characteristics of watersheds.

Coastal watersheds in southern California

In this study, we analyzed statistical relationships between freshwater discharge and plume size in four rectangular ocean regions in the near-shore zone of the SCB. Satellite-sensed visible spectral radiance (ocean color) data were obtained, processed, and analyzed within the part of each rectangular area (VE, SM, SP, and SD; Figure 1) providing ocean data. Each ocean region was associated with the group of coastal watersheds (Figure 1; Table 1), within which freshwater runoff originated, primarily from the water precipitated during rainstorms.

Rainfall and runoff patterns throughout the Southern California region are governed by a complex combination of atmospheric circulation and topographic effects. Low-pressure winter storms typically move southward from the North Pacific along the western edge of North America. As these

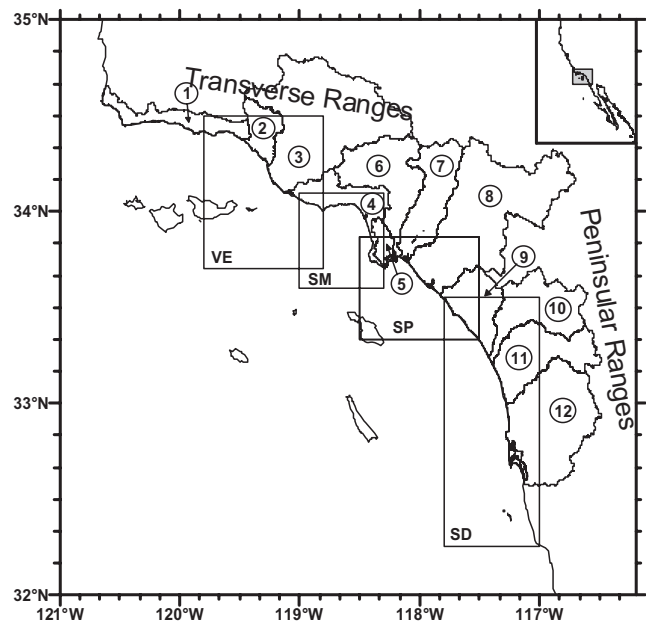


Figure 1. The scheme of the study area of the Southern California Bight. The rectangles in this figure indicate the areas of the regions where the plumes were analyzed: Ventura (VE), Santa Monica Bay (SM), San Pedro Shelf (SP), Orange County/San Diego (SD). The numerals in circles indicate the coastal watersheds where the rainstorm magnitude was estimated (Table 1).

Table 1. Coastal watersheds of the Southern California Bight.

#	Watershed	Area (km ²)
1	Santa Barbara Creek	971
2	Ventura River	696
3	Santa Clara River	5164
	Ventura region (total)	6831
	Malibu Creek	286
	Ballona Creek	338
4	Santa Monica Bay region (total)	1170
5	Dominguez Channel	300
6	Los Angeles River	2161
7	San Gabriel River	1758
8	Santa Ana River	5101
	San Pedro Shelf region (total)	9320
9	San Juan Creek	1284
10	Santa Margarita River	1915
11	San Luis Rey River/Escondido Creek	2002
12	San Diego River	3561
	Orange County/San Diego region (total)	8762

storm systems approach Southern California, they are moderated by the Pacific high-pressure system and a thermal low to the east, which deflects many storms (Bailey 1966). As a result, the average annual rainfall in Southern California is only 30 centimeters (12 inches), less than a third of the northern part of the California State (Beuhler 2003). During winter, the center of high pressure moves to a southwest position, allowing brief, intense Pacific storm fronts to penetrate the area (Lu *et al.* 2003). Rainfall patterns are further moderated by a temperature inversion created by the ring of mountain ranges that define Southern California. The east-west Transverse Ranges and the north-south Peninsular Ranges create a “coastal basin” where cool, dense air is trapped, often deflecting marine winds over the area, resulting in much weaker wind patterns than over the open ocean and lower rainfall than areas to the east (Dorman and Winant 1995).

Runoff from the Southern California coastal watersheds typically manifests as brief, intense episodes. Coastal watersheds are short and steep, dropping from almost 3000 meters in elevation to sea level, often in less than 200-km distance. The dynamic nature of runoff is exacerbated by land-use practices that are typical of most coastal areas. A population of approximately 20 million people is concentrated in a relatively narrow band of land

along the coastal plain (Schiff *et al.* 2000b). The impervious surfaces associated with these developed areas increase the magnitude and intensity of stormwater runoff, and associated loadings of contaminants, nutrients, and other pollutants, to the coastal ocean.

Although runoff from all Southern California coastal watersheds is influenced by the regional factors described above, there are some key differences between the four sub-regions. Differences that may affect runoff patterns are related to the trend of decreasing precipitation from the northern to southern watersheds (Beuhler 2003, Nezlin and Stein 2005) and the increasing role of the peninsular ranges in attenuating runoff from the southern watersheds.

The northern part of the SCB is associated with three watersheds, Santa Barbara Creek, Ventura River, and Santa Clara River. The largest is the 5164 km² Santa Clara River watershed. The Ventura River and Santa Barbara Creek watersheds are much smaller (696 and 971 km², respectively; Table 1). These watersheds are the least developed of the region (in terms of the percent of watershed area) and are dominated by forest, chaparral and coastal sage scrub. In addition, there is little hydrologic control in terms of major dams or flood control channels. The lack of hydrologic control combined with the typically higher rainfall compared to more southern watersheds, translates to high volumes of sediment-laden discharge following episodic rain events. Because the outlets of the Ventura and Santa Clara rivers are located close to each other (within 5 km), the discharges of these two rivers commingle and cannot be distinguished at 1.1-km resolution satellite images.

The Malibu and Ballona Creek watersheds, as well as several small watersheds draining the Santa Monica Mountains, discharge to SM. This area lies within the northern portion of the Transverse Ranges, which are characterized by very short and steep watersheds. Malibu Creek watershed is approximately 15% developed, with those areas concentrated in two portions of the watershed, which have been shown to produce high nutrient (Schiff and Bay 2003) and bacteria loads. With the exception of several tributaries, most of the creeks in the Malibu watershed are not channelized. In contrast, the Ballona Creek watershed is approximately 85% developed and the streams consist entirely of concrete channels or underground storm drains. The remaining short, steep watersheds draining the Santa Monica Mountains are mainly undeveloped.

The San Pedro Shelf receives discharge from four watersheds totaling 9320 km² of drainage area: Dominguez Channel, Los Angeles, San Gabriel, and Santa Ana rivers (Table 1). These four watersheds constitute the most populated areas of Southern California. Consequently, the streams are highly modified with numerous dams, diversions, and channels that tightly control runoff and have attenuated peak flows from historic levels (Dunne and Leopold 1978, Booth 1990). The greater Los Angeles basin is a series of overlapping floodplains ringed in mountains. In addition, this area was under water as recently as the Pleistocene period, less than 2 million years ago. The combination of marine and fluvial processes has resulted in a mix of marine and continental sedimentary materials that form deep alluvial aquifers along most of the coastal plain. Consequently, much of the surface runoff is diverted for ground water recharge prior to reaching the coast.

The southern-most Orange County/San Diego Region is associated with 12 major and several minor watersheds. The larger watersheds include San Diego Creek, San Juan Creek, Santa Margarita River, San Luis Rey River, Escondido Creek, and San Diego River watersheds. The total area of these coastal watersheds is 8762 km². This portion of the coast is distinct in that the watersheds generally drain to the west (as opposed to the south). This orientation contributes to drier and more temperate conditions than other portions of Southern California. In addition, the southern watersheds overlap both the Peninsular and Transverse Ranges resulting in bimodal longitudinal profiles. In the upper portions of the watersheds, water drains from the steep mountains of the transverse ranges to inland alluvial valleys. Water then flows down and across the lower peninsular ranges onto broad coastal terraces before discharging to the ocean. The inland valleys are often separated from the coastal terraces by steep, narrow gorges. This watershed physiography acts to attenuate water and sediment flow to the coast.

METHODS

Remotely-sensed normalized water-leaving radiation at 555-nm wavelength (nLw555; green-yellow band) was used to discriminate and contour freshwater plumes. Otero and Siegel (2004) showed that nLw555 is better correlated with the concentration of suspended sediments in near-surface waters than other wavelengths and, hence, is a good proxy for the water discharged from river

mouths after rainstorms. The nLw555 values were derived from SeaWiFS (McClain *et al.* 2004) data collected between October 6 (Julian Day 279) 1997 and June 26 (Julian Day 177) 2003. High-resolution (1.1-km) SeaWiFS Level 1A data were obtained from NASA's Goddard Space Flight Center Distributed Active Archive Center (GSFC DAAC; Acker *et al.* 2002) and processed using SeaDAS software (Version 4.3). To calculate nLw555 normalized water-leaving radiances (Level 2 data), near-coincident NCEP meteorological and EPTOMS and TOVS ozone data files were obtained from GSFC DAAC and applied to corresponding SeaWiFS Level 1A data. We used the standard SeaDAS algorithm with the "land", "cloud", and "stray light" flags among others applied as masks.

In each of the four study regions (Figure 1), nLw555 pixel values from each SeaWiFS scene were interpolated on a regular grid of spatial resolution 0.01°x0.01° (about 1 km). Missing data (MD) values were applied to the grid nodes located >2 km from the nearest non-missing pixel. The resulting images were visually analyzed to select the grids where clouds did not cover the coastal zone and the pattern of the freshwater plume was visible. Nevertheless, some of the selected images were partly covered by clouds. A stripe between the coast and the ocean also often contained MD because of the "stray light" mask effect. To quantitatively estimate the plume area at these images, we filled the ocean zones containing MD (i.e., covered by clouds) with interpolated nLw555 values. The grid nodes containing MD and located near the nodes with non-missing data (NMD) were replaced with the interpolated nLw555 values obtained by averaging the surrounding grid nodes using a 3x3 Gaussian filter. Each step of this operation added NMD at the edge between the NMD and MD, areas covered by clouds. This operation was repeated until all grid nodes in the ocean zone were filled with NMD. Land masks were applied to the grids to remove (i.e., replace by MD) the data unintentionally interpolated over the land. This iterative process was visually controlled to avoid a substantial distortion of plume contour; if this happened, the image was removed from the analysis.

The total number of analyzed SeaWiFS scenes (October 1997 - June 2003) was 493 in the VE region, 268 in the SM region, 628 in the SP region, and 320 in the SD region. During other days no SeaWiFS observations were obtained due to cloudy weather/no available data over the SCB. In each

scene, the plume area was estimated on the basis of the area covered by waters with high nLw555 index. The level of nLw555 indicator value to distinguish between the plume and the ambient waters was initially unknown; the goal of the study was to select the nLw555 indicator which best characterizes the plume boundary in different regions. For this, we tested the “plume boundary” threshold levels within the range from 0.5 to 2.0 mW cm⁻² μm⁻¹ sr⁻¹; the nLw555 level bounding the plume area that best correlated with stormwater discharge was selected as a plume indicator.

Rainstorm magnitude was estimated from the atmospheric precipitation averaged over four combined watersheds related to the four study regions (Figure 1; Table 1). Daily rain gauge data from 98 meteorological stations located in these watersheds were downloaded from the National Oceanic and Atmospheric Administration (NOAA) National Data Center Climate Data Online (NNDC/CDO) website. Each observation represents the precipitation during a 24-hour period preceding the observation time. The precise time of observation varied between the stations during different periods; therefore, we attributed each observation to an entire day and did not analyze the variability at a sub-diurnal time-scale. Not all stations had continuous data for the entire 6-year period of analysis; so, the average precipitation for each day from October 1997 till June 2003 was estimated from a variable number of stations (see details in Nezlin and Stein 2005).

The analysis of correlation between the rainstorm and the plume area is based on the model of linear “signal/response” dependence between these two parameters. To obtain a quantitative statistical evaluation of the response of the plume size as estimated by an area occupied by water with nLw555 exceeding the selected threshold to the rainstorm signal, we calculated the time-lagged linear Pearson correlation coefficients between the plume area and the rainstorm magnitude. Different levels of nLw555 were used to find maximum correlation between plume area and rainstorm; the nLw555 resulting in maximum correlation was considered as best plume edge indicator.

To evaluate the persistence of the rainstorm signal in the plume area we estimated for each (*t*th) day the precipitated water volume (*V_t*) accumulated during the previous period by the day preceding the plume, using the equation:

$$V_t = \sum_{i=1}^{t-1} k^{t-i} \cdot P_i = P_{t-1} + k \cdot P_{t-2} + k^2 \cdot P_{t-3} + k^3 \cdot P_{t-4} + k^4 \cdot P_{t-5} + \dots \quad (1)$$

where *P_i* is the precipitation during the *i*th day and *k* is the coefficient of persistence of the freshwater plume. The coefficient of persistence, for 0 < *k* < 1 each day, represents the *k*th part of the water accumulated during the preceding period is retained in the plume and the 1-*k*th part is dissipated. The values of *k* within the range 0.05 - 0.95 were tested to obtain best correlation between *V_t* and the plume area.

To describe typical plume patterns, we estimated the zones where the plumes occurred after rainstorms of different magnitude. Rainstorms were classified into five gradations: <0.25 cm; 0.25 - 0.6 cm; 0.6 cm - 1 cm; 1 - 2.5 cm; and >2.5 cm of accumulated precipitated water (Equation 1), using the coefficient *k* resulting in best correlation between rains and plumes in that region. Similar classification of rainstorms (<0.25 cm; 0.25 - 0.6 cm; 0.6 - 2.5 cm; and >2.5 cm) was used by Ackerman and Weisberg (2003) studying stormwater discharge to the Santa Monica Bay; we added one more gradation splitting the gradation 0.6 - 2.5 cm into two (0.6 - 1 cm and 1 - 2.5 cm). For our classification we used accumulated water rather than the magnitude of each rainstorm. The basis of our approach was to avoid the difficulties of the analysis of situations when two or more rainstorms follow each other (a relatively frequent occurrence). The duration of rainstorms in Southern California is short, typically 6 - 12 hours (Schiff *et al.* 2000a); therefore, we do not expect much difference between the values of accumulated precipitation (Equation 1) and total precipitation for a rainstorm that immediately follows a prior rain event. To illustrate the plume patterns in terms of the statistical theory of probability, we estimated for each grid node the percentage of images when this node was attributed to plume. The resulting composites were smoothed by 5-km 2D cosine-filter.

To describe the physiographic differences between watersheds, we used the Digital Elevation Model (DEM) GTOPO30 (USGS 1996) with a horizontal grid spacing of 30 arc seconds (approximately 1 km). The elevations of the DEM grid nodes within the land area of each of four regions (Figure 1) were tabulated and presented as histograms.

Land cover/land use data were developed using 30-meter resolution LandSat satellite imagery provided by the NOAA Coastal Services Center. These

data separate the area into 39 land types based on the standard 22 NOAA Coastal Change Analysis Program (C-CAP) land cover categories. Land use/land cover classifications are based on year 2000 imagery. We distinguished between six categories of land use:

- 1) Developed land (both high intensity and low intensity);
- 2) Cultivated land;
- 3) Grassland (both managed and naturally occurring);
- 4) Forests and parks (including deciduous, evergreen, and mixed);
- 5) Scrubs and shrubs; and
- 6) Wetlands.

In each region we estimated the proportion of the total area occupied by each land-use category.

RESULTS

An important issue concerning rainstorm plume dynamics is the time lag between the rainstorm and the resulting plume. Statistical analysis of the time series of precipitation and plume size collected during almost six years of observations (October 1997 - June 2003) shows that the time lags between rainstorms and plumes were different in different regions. We explored the correlation between the plume areas estimated from different nLw555 and the daily precipitation averaged over the watersheds of each region (Figure 2). In three regions (VE, SM, SD), maximum correlation was observed on the second day after rainstorm. Over the San Pedro Shelf, maximum correlation was observed at the first day. The nLw555 values resulting in maximum correlation and, hence, best indicating the plume boundary, were also different in different regions. In the SM region, nLw555 was low, ranging from 0.8 to 1.0 $\text{mW cm}^{-2} \mu\text{m}^{-1} \text{sr}^{-1}$; in the SD region, nLw555 ranged between 1.2 and 1.3 $\text{mW cm}^{-2} \mu\text{m}^{-1} \text{sr}^{-1}$; in the VE region and over the San Pedro Shelf, a wide range of nLw555 coefficients, from 1.2 to 1.9 $\text{mW cm}^{-2} \mu\text{m}^{-1} \text{sr}^{-1}$, resulted in high correlation with stormwater. The maximum correlation coefficient was lowest (+0.39) in the SM region and higher in the SD (+0.43) and VE (+0.49) regions. The highest correlation was observed over the San Pedro Shelf (+0.53).

The persistence of plumes (i.e., the time during which plumes were observed after each rainstorm) was varied among the four regions. Introducing k (Equation 1), we focused on the concept that esti-

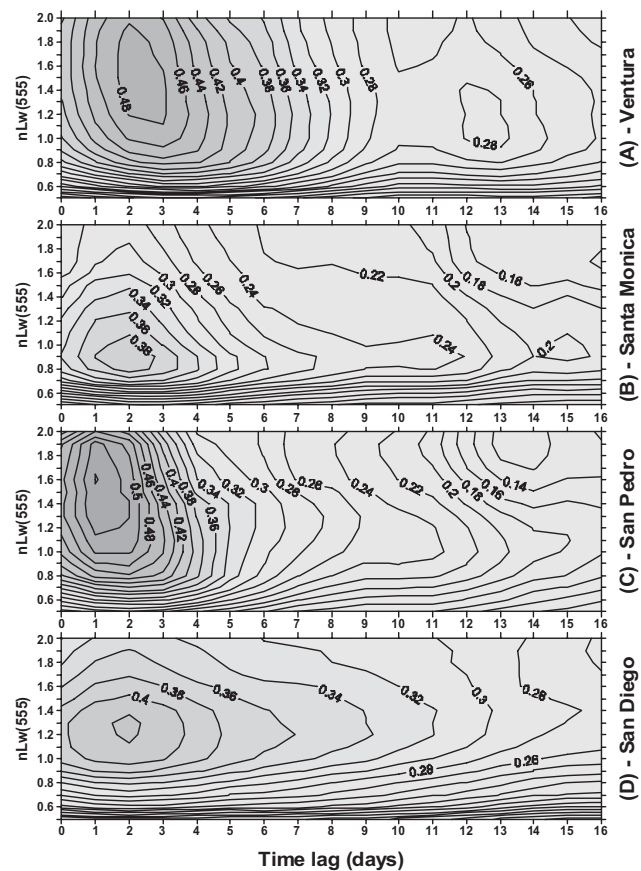


Figure 2. 2D-diagrams of the correlations between the freshwater plume areas (bounded by different nLw 555 levels) and the rainstorm magnitudes in the adjacent watersheds at different time lags.

imating the correlation between precipitation and plume area, we should take into account not only the stormwater precipitated during the last rainstorm, but the antecedent precipitation as well. To do so, we transformed the precipitation over the watersheds of each of four study regions using Equation 1 for k within the range of 0.05 to 0.95. We estimated the correlation coefficients between the transformed precipitation and the plume areas bounded by different nLw555 within the range of 0.5 to 2.0 $\text{mW cm}^{-2} \mu\text{m}^{-1} \text{sr}^{-1}$. In all four regions, the correlation diagram showed one evident maximum; plume boundary nLw555 and accumulated stormwater coefficients of persistence were used to estimate the plume/rain relationship (Figure 3; Table 2). In the VE, SP, and SD, the nLw555 resulting in a maximum correlation was 1.2 to 1.3 $\text{mW cm}^{-2} \mu\text{m}^{-1} \text{sr}^{-1}$; in the SM region, it was much lower (0.8 $\text{mW cm}^{-2} \mu\text{m}^{-1} \text{sr}^{-1}$). So, we considered the nLw555 indicating plume boundaries to be 0.8 $\text{mW cm}^{-2} \mu\text{m}^{-1} \text{sr}^{-1}$ in the SM region and 1.2 to 1.3 $\text{mW cm}^{-2} \mu\text{m}^{-1} \text{sr}^{-1}$ in three other regions. In the VE, SM, and SP regions, k ranged between

Table 2. Statistical characteristics of the maximum correlations between freshwater plume areas and accumulated stormwater.

Region	nLw555 (mW cm. ² μm. ⁻¹ sr. ⁻¹)	k (coefficient of plume persistence; Equation 1)	Maximum correlation (R)
Ventura	1.3	0.89	0.7995
Santa Monica Bay	0.8	0.9	0.7981
San Pedro Shelf	1.3	0.75	0.8516
Orange County/ San Diego	1.2	0.9	0.6432

0.89 and 0.90; over the San Pedro Shelf, *k* was much lower (0.75).

The relationships between accumulated stormwater and plume area size (estimated on the basis of the optimal time lag, nLw555, and *k*) were analyzed in four regions (Table 3; Figure 4). Plume boundary nLw555 and accumulated stormwater *k* used to estimate the plume/rain relationship are given in Table 2, correlation coefficients are given in Table 3. The intercepts of all four linear equations were insignificantly different from zero. Zero intercept indicates that at zero rainstorm, the size of plume was negligible, i.e., no plume was detected by satellite. At the same time, the slopes of the linear equations were different, indicating that in different regions similar rainstorm magnitude resulted in different plume response. The most prominent response was observed in the Ventura region (1 cm of accumulated stormwater resulted in

plume size ~130 km²). In the SM and SP regions, 1 cm of rainfall resulted in a plume size of 90 - 94 km². Notably, in the SM region, plumes were detected by an nLw555 of 0.8 mW cm.⁻² μm.⁻¹ sr.⁻¹;

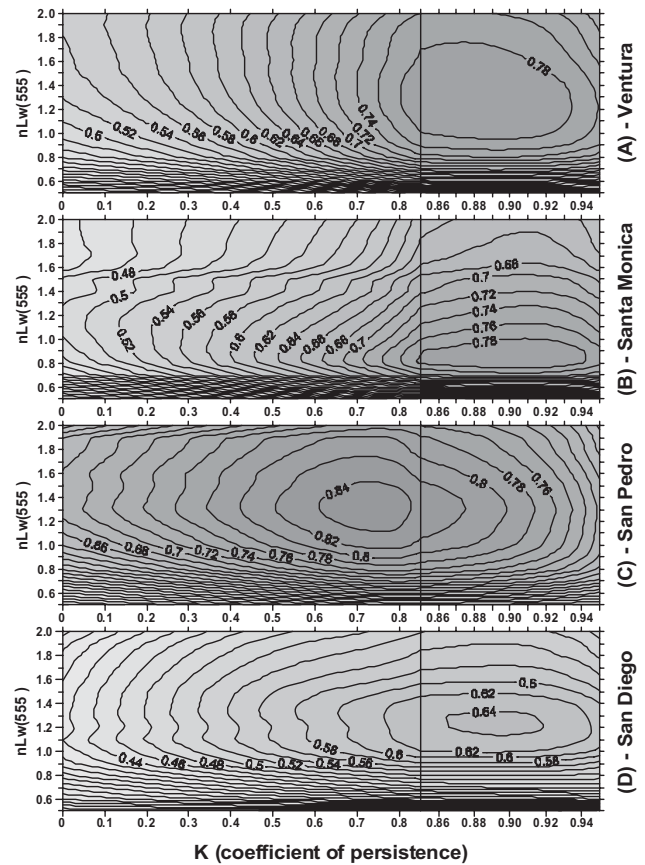


Figure 3. 2D-diagrams of the correlations between the freshwater plume areas bounded by different nLw555 levels (Y-axis) and the precipitated water accumulated over the adjacent watersheds and estimated with different coefficients of persistence (*k*, X-axis). Note the change of the scale of X-axis at 0.85.

Table 3. Coefficients and the analysis of variance of linear (Y=A+B*X) and power (Y=C*X^D) regression equations between accumulated stormwater (X) and plume area (Y).

	REGION			
	Ventura	Santa Monica Bay	San Pedro Shelf	Orange County/ San Diego
Time lag (days)	2	2	1	2
Linear equation	Y=-5.63+130.22*X	Y=-11.13+89.68*X	Y=2.96+94.19*X	Y=1.10+52.00*X
Plume variability explained by linear equation (%)	65.4	64.9	72	42.3
F (d.f.)	926.0 (1,490)	489.8 (1,265)	1613.4 (1,626)	232.7 (1,317)
p	0.0	0.0	0.0	0.0
Power equation	Y=61.92*X^1.4035	Y=23.14*X^1.6486	Y=73.62*X^1.1559	Y=20.20*X^1.6807
Plume variability explained by power equation (%)	75.1	77.9	76.5	58.2
F (d.f.)	739.7 (2,490)	468.4 (2,265)	1021.3 (2,626)	220.9 (2,317)
p	0.0	0.0	0.0	0.0

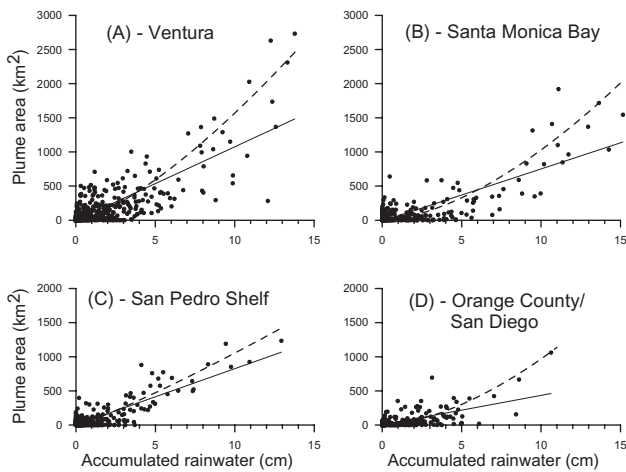


Figure 4. Linear (solid line) and power (dashed line) relationship between accumulated stormwater and plume area.

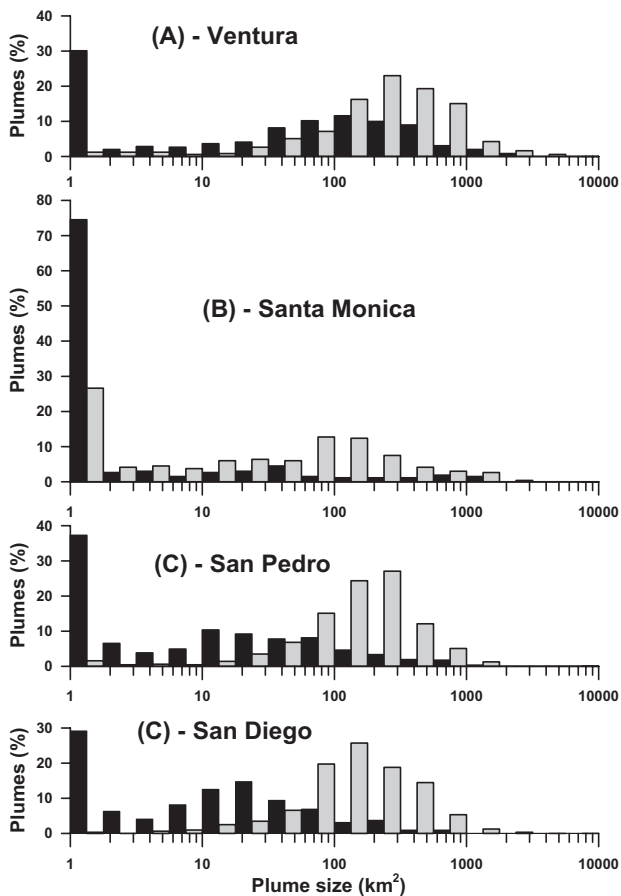


Figure 5. Size frequency distribution (%) of plume areas observed between September 1997 and June 2003. Black and grey bars indicate plume areas bounded by nLw555 levels 1.3 and 0.8 mW cm⁻² μm⁻¹ sr⁻¹, respectively.

whereas, over the San Pedro Shelf the nLw555 was 1.3 mW cm⁻² μm⁻¹ sr⁻¹. In the SD region, the relationship was least prominent (~52 km² of plume size per 1 cm of rainfall).

The difference between the slopes of the linear equations became more dramatic after each slope coefficient was normalized to drainage area. For plumes estimated from nLw555 = 1.3 mW cm⁻² μm⁻¹ sr⁻¹, the ratio between plume size produced by 1 cm of rainfall and drainage area was largest in the VE region (0.019); half as large in the SP region (0.010); and lowest in the SD region (0.006). The similar ratio for the SM region (0.077) could not be compared to the other three regions, because plumes there were detected by lower nLw555 (0.8 mW cm⁻² μm⁻¹ sr⁻¹).

Power equations described plume/rain relationship better than the linear relationships in all four regions (Table 3). In the SP region, the power coefficient (1.156) was close to 1 and the power equation did not differ much from the linear one (Figure 4C). In the three other regions, the power coefficients (1.40 - 1.68) were significantly higher than 1 and the power equations more accurately represented the relationship between the accumulated stormwater and the plume area size (Figure 4A, B, and D).

Plume areas were different in each of the four study regions (Figure 5), varying according to the level of nLw555 indicator used. The optimal nLw555 levels indicating plume boundaries was 0.8 mW cm⁻² μm⁻¹ sr⁻¹ in the SM region and 1.2 - 1.3 mW cm⁻² μm⁻¹ sr⁻¹ in the three other regions. To compare the plume areas characteristics of these different regions, we used nLw555 values of 0.8 and 1.3 mW cm⁻² μm⁻¹ sr⁻¹. When the plume was bounded by nLw555 = 0.8 mW cm⁻² μm⁻¹ sr⁻¹ in the VE, SP, and SD regions, the plume size distributions were unimodal with maxima at 80 - 1000 km². In these three regions, plumes (i.e., the zones of nLw555 > 0.8 mW cm⁻² μm⁻¹ sr⁻¹) were observed in almost all scenes, during both wet and dry weather. The plumes in the VE and SP regions were largest (typical size = 150 - 200 km²); in the SD region, plumes were smaller (100 - 150 km²). The plume size distribution in the SM region was bimodal. The most frequently occurring plume size was < 2 km² (i.e., no plume); the second maximum of size distribution was at 50 - 150 km².

When the plumes were bounded by nLw555 = 1.3 mW cm⁻² μm⁻¹ sr⁻¹, the plume size distributions were bimodal in all four regions. The most frequent

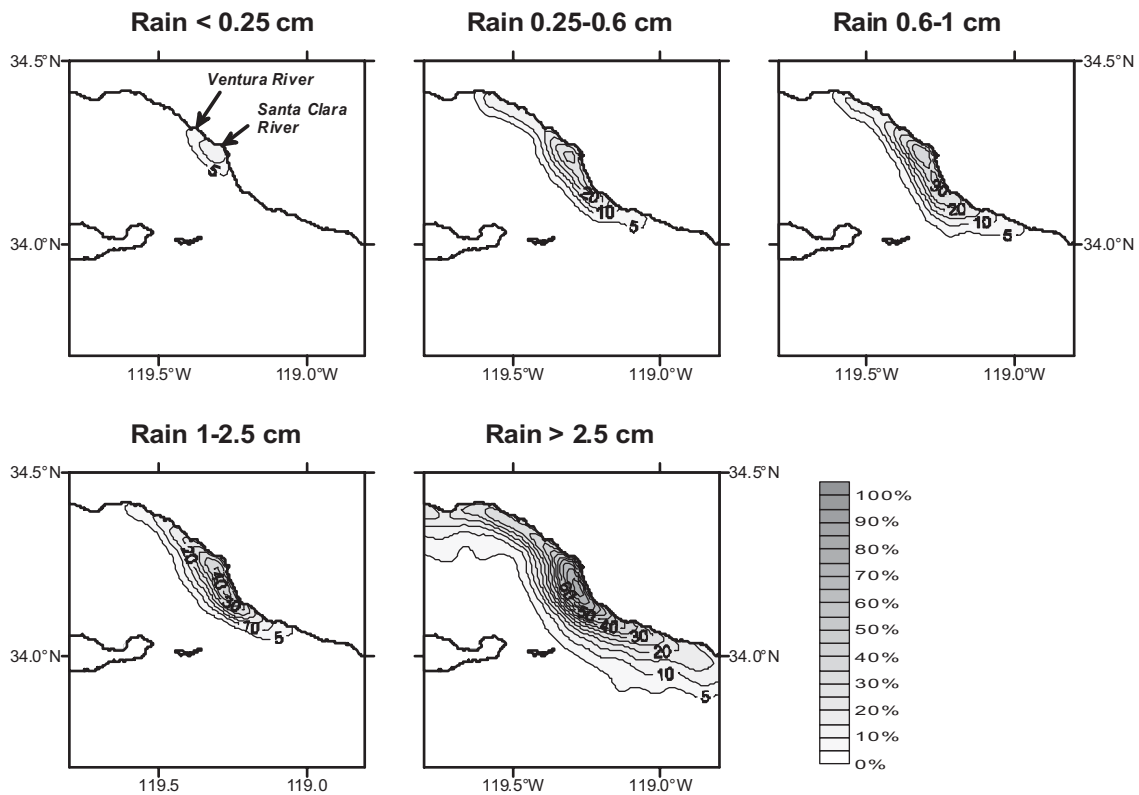


Figure 6. The areas occupied by freshwater plumes after rainstorms of different magnitude in Ventura region.

plume size was $<2 \text{ km}^2$. That is, for 29% - 37% of the images of the VE, SD, and SP regions and 74% of the images of the SM region, no plume was observed. The second maximum of size distribution indicated plumes observed after rainstorms. Largest plumes were observed in the VE region (100 - 150 km^2). In the SM region, the second maximum was related to plume size 30 - 60 km^2 ; however, the number of images with observable plumes was very small (4.5%). Over the San Pedro Shelf, plume sizes ranged between 10 and 100 km^2 . In the SD region, typical plume size was 5 - 40 km^2 .

The size of plume area bounded by $nLw555 > 1.3 \text{ mW cm}^{-2} \mu\text{m}^{-1} \text{ sr}^{-1}$ increased with rain magnitude in all four regions. In the VE region during dry periods (rain $<0.25 \text{ cm}$), plumes occurred only in the mouths of Santa Clara and Ventura rivers at 10% - 15% of scenes (Figure 6). In these graphs, the iso-lines indicate the percentage of satellite images with $nLw555 > 1.3 \text{ mW cm}^{-2} \mu\text{m}^{-1} \text{ sr}^{-1}$; the resulting grids were smoothed by 5-km cosine-filter. After small and medium rainstorms (0.25 - 2.5 cm) plumes near the river mouths were observed at $>50\%$ of scenes. Plumes propagated in both directions along the coast; the occurrence of plumes gradually decreased with the distance from river mouth. When the rain-

storm exceeded 2.5 cm, the plume zone was observed along the entire coast and was much wider offshore. The plume pattern was symmetrical; no preference in plume propagation (poleward vs. equatorward) was detected.

In the SM region, after rainstorms ($<2.5 \text{ cm}$), plumes bounded by $nLw555 > 1.3 \text{ mW cm}^{-2} \mu\text{m}^{-1} \text{ sr}^{-1}$ were so small that could not be readily detected from satellite observations. However, after heavy rains ($>2.5 \text{ cm}$), plumes bounded by $nLw555 > 1.3 \text{ mW cm}^{-2} \mu\text{m}^{-1} \text{ sr}^{-1}$ did occur along the entire local coast, with the frequency of plume occurrence decreasing rapidly offshore (Figure 7F). As such, the apparent influence of rainstorms on the optical properties of surface waters in the SM region was seemingly not as great as in the other regions. The best correlation between precipitated stormwater and plume area was observed when the plume threshold was smaller ($nLw555 > 0.8 \text{ mW cm}^{-2} \mu\text{m}^{-1} \text{ sr}^{-1}$) as compared with the VE, SP, and SD regions ($nLw555 > 1.3 \text{ mW cm}^{-2} \mu\text{m}^{-1} \text{ sr}^{-1}$). Within the SM region, when the plumes were bounded by $nLw555 = 0.8 \text{ mW cm}^{-2} \mu\text{m}^{-1} \text{ sr}^{-1}$, even during dry periods (accumulated precipitation $<0.25 \text{ cm}$), small plumes were observed inshore at 5 - 10% of scenes (Figure 7A). After rainstorms 0.25 - 2.5 cm, plumes occurred more frequently, with

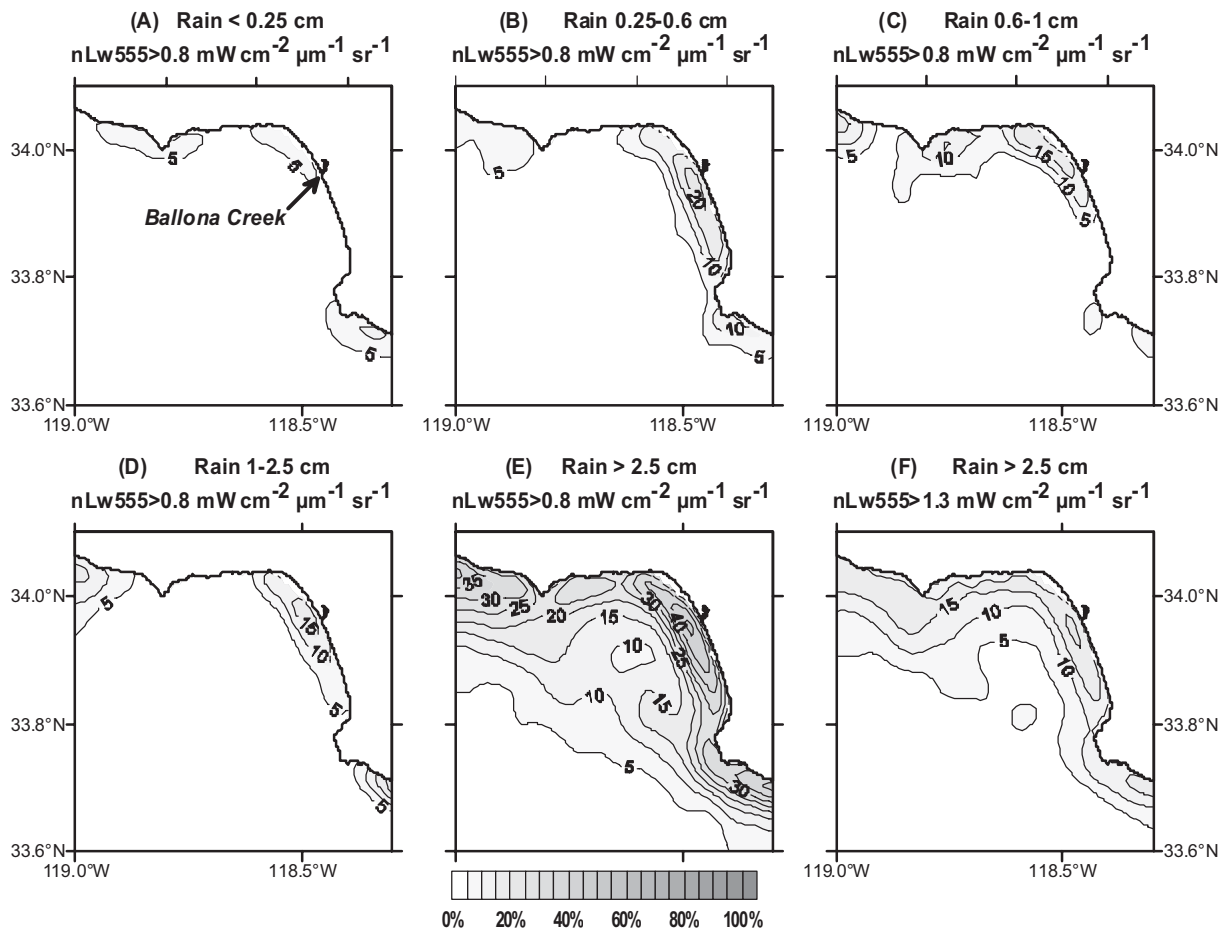


Figure 7. The areas occupied by freshwater plume after rainstorms of different magnitude in Santa Monica Bay.

a maximum occurrence near the mouth of Ballona Creek (Figure 7B - D). After strong rainstorms (>2.5 cm), the entire SM region was covered by plumes; near the mouth of Ballona Creek, plumes were observed in >50% of scenes (Figure 7E).

In the SP region, dry season (rain <0.25 cm) plumes were observed 10 - 15% of the time at the mouth of the Los Angeles and San Gabriel Rivers (Figure 8). The width of the zone where plumes were observed and the frequency of plumes increased with increasing rainstorm magnitude. After rains >2.5 cm, plumes were observed at almost all occasions along the coast from the mouth of Los Angeles River to the mouth of Santa Ana River. Plumes often propagated offshore in the south-southeastern direction.

In Orange County/San Diego region, plumes frequently (20% - 25% of scenes) occurred in the small zone near the mouth of San Diego Bay (Figure 9) during both dry season and after rainstorms <1.0 cm. After rainstorms 1.0 - 2.5 cm, the frequency of plumes in this zone increased by 40% - 50%; small plumes were also observed along the

San Juan Creek watershed. After strong rainstorms (>2.5 cm), plumes were observed at almost all occasions near San Diego Bay and at 10% - 20% of the time near the mouth of the San Juan Creek watershed, and to the south of San Diego Bay.

The elevation characteristics of all four watersheds were different (Figure 10). In the watersheds adjacent to Santa Monica Bay, the terrain was substantially lower as compared with VE, SP, and SD regions. In the Santa Monica Bay watershed, >30% of the terrain was <100 m high (Figure 10B); the elevation of most of the remaining area did not exceed 500 m. In the watershed adjacent to San Pedro Shelf about 15% of the terrain was <50 m (Figure 10C). At the same time, 40% of the area of the watersheds adjacent to San Pedro Shelf exceeded 500 m. However, it is important to keep in mind that the total area of the watersheds draining to the San Pedro Shelf (i.e., Los Angeles, San Gabriel, and Santa Ana Rivers) is almost an order of magnitude greater than the watershed area draining to Santa Monica Bay (Table 1). The elevation in the northern region

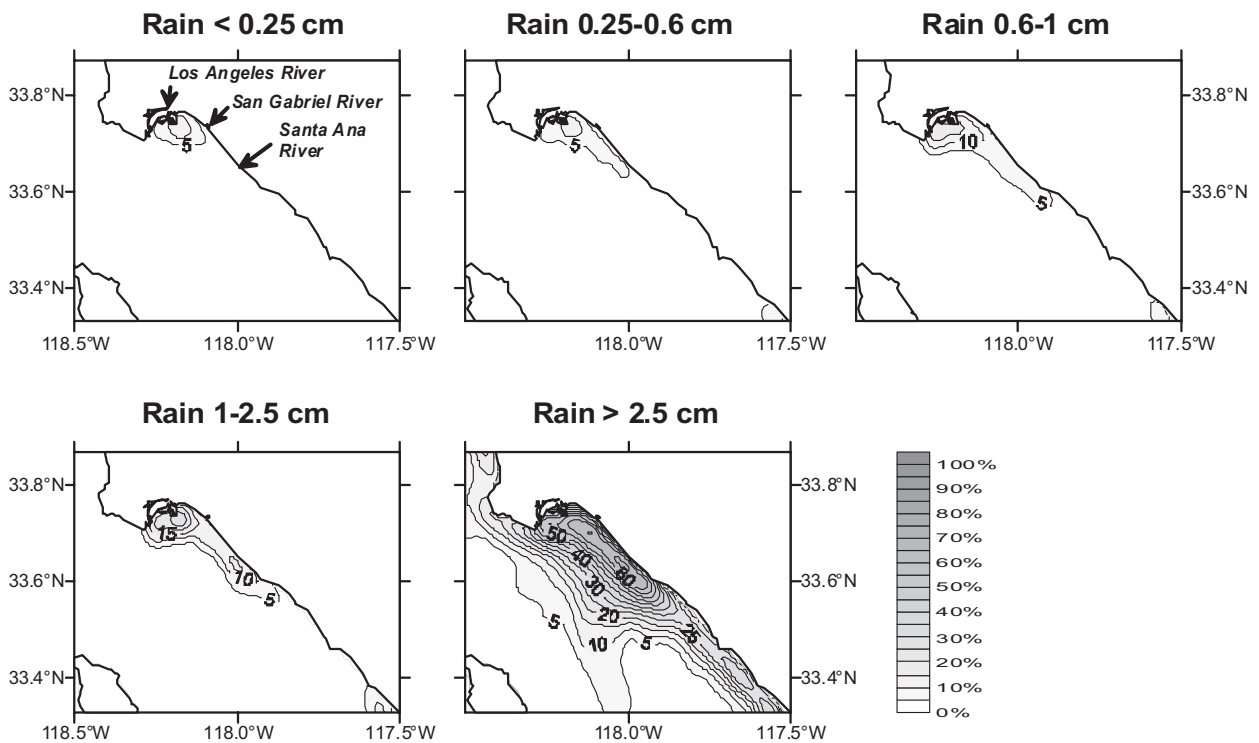


Figure 8. The areas occupied by freshwater plumes after rainstorms of different magnitude over San Pedro Shelf. The isolines indicate the percentage of satellite images with $nLw_{555} > 1.2 \text{ mW cm}^{-2} \mu\text{m}^{-1} \text{ sr}^{-1}$; the resulting grids were smoothed by 5-km cosine-filter.

(Ventura, Figure 10A) was higher than in the other two regions; almost 30% exceeded 1000 m (cf., 21% in San Pedro, 15% in Orange County/San Diego, and 0% in Santa Monica Bay).

Land use characteristics differed between the regions. Watersheds draining to the SP region, and to a lesser extent to the SM region, are densely populated and urbanized. In contrast, watersheds draining the VE and SD regions are less populated and contain more undisturbed area. About 40% of the watersheds adjacent to Santa Monica Bay and San Pedro Shelf were covered by impervious surfaces (Figure 11B, C). In contrast, the impervious cover in the VE (Figure 11A) and SD (Figure 11D) regions was much lower (7% - 14%). The total area of pervious land (grasslands, forests, and shrubs) was 58% - 61% in SM and SP regions and 81% - 85% in VE and SD regions.

DISCUSSION

Backscattering index as a plume indicator

High correlation between accumulated stormwater and the areas of river plumes estimated on the basis of backscattering index (i.e., normalized water-leaving radiance of 555-nm wavelength nLw_{555} ; green-yellow band) indicates that the lat-

ter optical property is a good proxy of the amount of freshwater discharged to coastal ocean. This conclusion agrees with the results of previous studies. Otero and Siegel (2004) studying freshwater plumes in the northern part of the SCB showed that the SeaWiFS 555-nm band is better correlated with the concentration of suspended sediments than other bands. Toole and Siegel (2001) have shown that nLw_{555} was highly correlated with lithogenic silica concentration, which, in turn, is an important constituent of river discharge and was found to be a good indicator of suspended sediment concentration (Shipe *et al.* 2002; Warrick *et al.* 2004b).

The level of nLw_{555} , which exceeded $1.3 \text{ mW cm}^{-2} \mu\text{m}^{-1} \text{ sr}^{-1}$ was found to be a good indicator of river plumes in all study regions excluding SM. A similar value was noted earlier by Otero (2002) for the Santa Barbara Channel in the northern part of the SCB and by Nezlin and DiGiacomo (2005) over the San Pedro Shelf. We hypothesized, however, that high nLw_{555} can result not only from the runoff-discharged high sediment concentration, but also from high chlorophyll concentration related to elevated phytoplankton biomass (Kirk 1994).

Otero (2002) and Toole and Siegel (2001) analyzed the nLw_{555} values in the mouth of the Santa

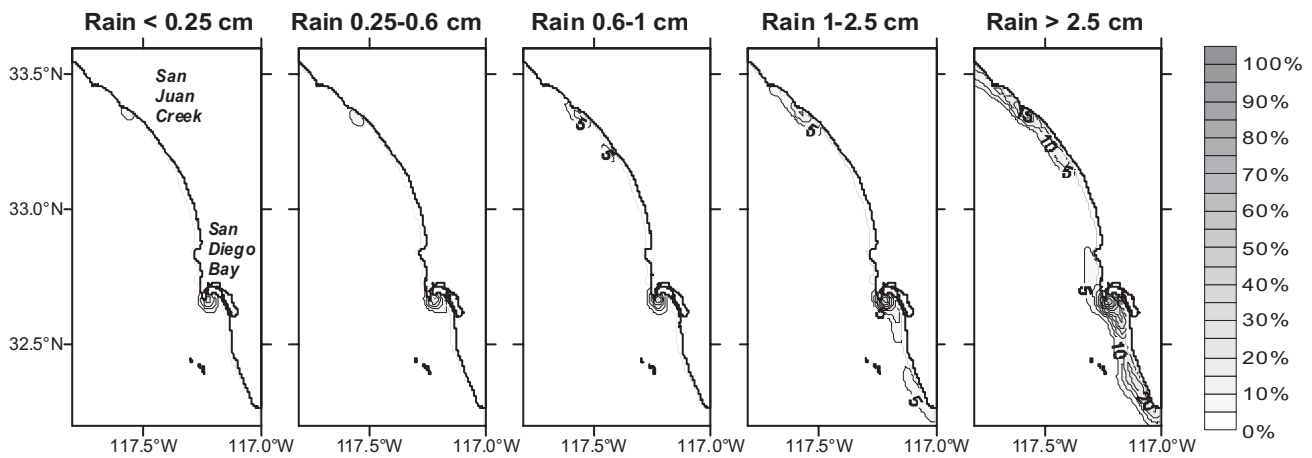


Figure 9. The areas occupied by freshwater plume after rainstorms of different magnitude in Orange County/San Diego region. The isolines indicate the percentage of satellite images with $nLw\ 555 > 1.2\ mW\ cm^{-2}\ \mu m^{-1}\ sr^{-1}$; the resulting grids were smoothed by 5-km cosine-filter.

Clara River in 1997 - 2001 and showed that under high chlorophyll concentration ($>2\ mg\ m^{-3}$) $nLw555$ also increased but never exceeded $1.0 - 1.3\ mW\ cm^{-2}\ \mu m^{-1}\ sr^{-1}$. At the same time, within the Santa Clara River plume, $nLw555$ was much higher ($4.6 - 11.1\ mW\ cm^{-2}\ \mu m^{-1}\ sr^{-1}$). A close agreement between the results of earlier studies and our observations provides a basis for recommendation to use $1.3\ mW\ cm^{-2}\ \mu m^{-1}\ sr^{-1}$ as an indicator of the boundary of freshwater plumes off Southern California.

In this study, we focused on the correlation between stormwater and plume areas using indicator $nLw555$ values as a representative proxy, avoiding quantitative estimations of the concentration of suspended sediments. However, recent methodological studies provide an opportunity for evaluation of the amount of suspended sediments from satellite data (Acker *et al.* 2004, Miller and McKee 2004, Warrick *et al.* 2004a). A comparison between these estimations and the results of the modeling of sediment and pollution discharge to the SCB (Ackerman and Schiff 2003, Ackerman *et al.* 2005) will be a focus of our future work.

Quantitative relationship between accumulated stormwater and plume area

The “accumulated stormwater” index estimated from daily rainfall (Equation 1) is a better predictor of plume area than daily rainstorm magnitude. Consequently, it should be more useful to managers in making decisions regarding beach postings or closures. In all four regions we studied, the coefficients of determination (R^2) of rain/plume linear correlation appeared to be substantially higher after

the time-series of precipitated water was transformed to “accumulated stormwater” using Equation 1. Rainstorms in Southern California are short episodic events. At the same time, the resulting plumes emerge during 1 - 2 days after the rainstorms and persist for several days, if not weeks. Transforming rainstorm time-series with Equation 1 dramatically decreases its temporal variability, making its autocorrelation function similar to the autocorrelation function of plume dynamics (Nezlin and DiGiacomo 2005). Estimating the “accumulated stormwater” index from daily precipitation, we take into account all antecedent rainstorms, weighting their contribution according to the time period between the rainstorm and the plume.

Zero intercept in linear regression equations between the accumulated stormwater and the size of plume area indicates that rainfall was a primary source of the plumes observed in the SeaWiFS data set. The assumption that a substantial portion of stormwater was infiltrated and accumulated in the soil and in reservoirs would have resulted in negative intercept of linear regression (i.e., precipitation lower than some threshold was retained in the watersheds; only the stormwater exceeding this threshold flowed to the coastal ocean and produced plumes). An alternative hypothesis that the satellite-observed plumes were produced by factors other than stormwater (e.g., year-round domestic wastewater discharge, wind-driven sediment resuspension, phytoplankton blooms, etc.) would have resulted in positive intercept (i.e., plumes existed even in the absence of rainstorms). However, in all four regions the intercepts of linear equations were insignificantly differ-

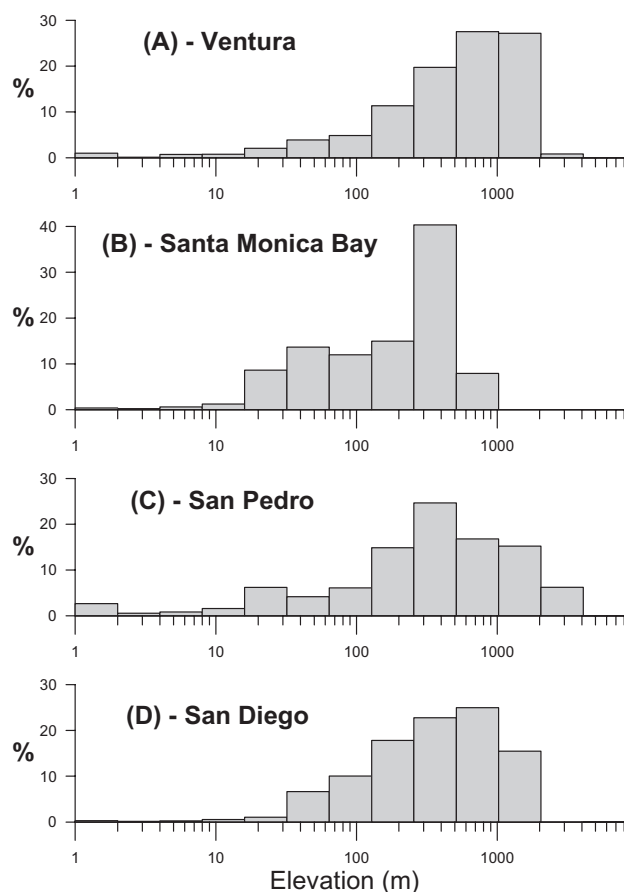


Figure 10. Percentage of elevations in watersheds.

ent from zero, indicating rainfall as a most likely source of plumes along the Southern California coast. We should keep in mind, however, that zero intercepts of the linear equations can partly result from the scatter in the data, particularly at the low end of the scale (i.e., small rain events); R^2 being within the range 0.42 - 0.72 (Table 1). In particular, plumes with $nLw_{555} > 1.3 \text{ mW cm}^{-2} \mu\text{m}^{-1} \text{ sr}^{-1}$ (or $> 0.8 \text{ mW cm}^{-2} \mu\text{m}^{-1} \text{ sr}^{-1}$ in Santa Monica Bay) were often observed at zero precipitation, including dry periods (Figure 4) and can be explained by release of water from reservoirs and sediment resuspension. Also, zero plume areas were often observed after significant precipitation, which can be explained by water retention in reservoirs. These positive and negative residuals counterbalanced each other, resulting in zero intercepts.

Wind-driven sediment resuspension was not likely to be a source of increased nLw_{555} values in the SCB. Washburn *et al.* (1992) studied this process in the western part of San Pedro Shelf and observed high concentrations of sediments resuspended by water circulation only within 15 m of the bottom. In

all the study regions here the ocean bottom exceeded 15 m within 1 km offshore; as such, the sediments resuspended from the bottom by winds, waves, and currents were not likely to be a significant factor for purposes of these analyses.

Continuous freshwater discharge from municipal waste sources cannot produce prominent nearshore plumes along the coast of Southern California (Svejkovsky and Jones 2001). Eganhouse and Venkatesan (1993) and Steinberger and Stein (2004) estimated the amount of this discharge as $1.4 - 1.6 \times 10^9 \text{ m}^3 \text{ year}^{-1}$, which is equal on the average to $3.8 - 4.4 \times 10^6 \text{ m}^3 \text{ day}^{-1}$. At the same time, even a minor rainstorm of 0.25 cm produces about $36 \times 10^6 \text{ m}^3$ of freshwater discharge to the SCB. This value is a product of precipitation times the total area of the coastal watersheds, after removal of the watershed area upstream of dams, which is 14652 km^2 (Ackerman and Schiff 2003). A moderate rainstorm of 1 cm produces a discharge that exceeds the municipal wastewater discharge by more than one order of magnitude. Freshwater runoff from storm events is primarily discharged to the coastal ocean during the first 1 - 2 days post-event, transporting significant loadings of suspended sediments whose concentration is especially high during the first few hours of the flux (Bertrand-Krajewski *et al.* 1998, Cristina and Sansalone 2003). As such, the mass of sediments transported to the ocean during rainstorms is several orders of magnitude higher than during dry periods (Mertes and Warrick 2001), and these sediments manifest themselves in large plumes that can be observed remotely from satellite platforms based on their optical signatures as described here.

In Southern California, it is clear that a substantial portion of stormwater runs off the coastal land mass and is discharged to the adjoining ocean, contributing to plume formation. In a previous study in the San Pedro Shelf region, Nezlin and DiGiacomo (2005) estimated that the total amount of precipitated stormwater was close to the total amount of discharged freshwater producing the plume, based on the coefficients of a linear “rain/plume” equation, the size of watershed area, and published measures of plume salinity. In this study, we showed that the relationship between stormwater and plume size could be described by a linear equation with zero intercept not only on the San Pedro Shelf, but also in other regions of Southern California as well. Hence, the speculations of Nezlin and DiGiacomo (2005)

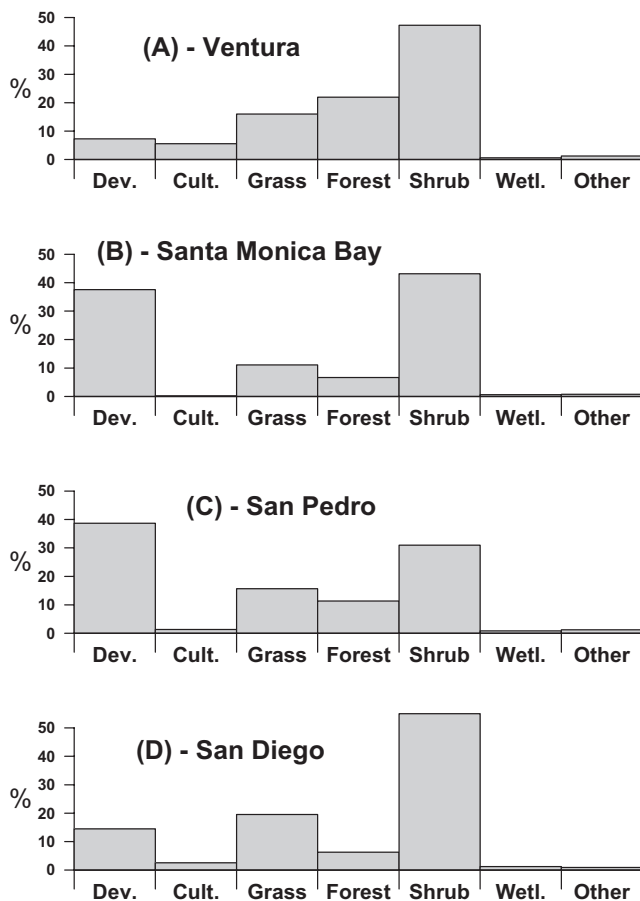


Figure 11. Percentage of various land-use areas in watersheds: developed land (Dev.); cultivated land (Cult.); grasslands (Grass); deciduous, evergreen and mixed forests (Forest); scrub/shrub areas (Shrub); wetlands (Wetl.), and other uses (Other).

are likely applicable to all coastal regions of Southern California. The slopes of the linear equations from this study vary within the range of 52 - 130 (Table 3), which differs from the slope coefficient of the equation estimated for San Pedro Shelf (94.2) by $\pm 50\%$. As such, the size of the plume area in the Ventura region was more than twice the plume size produced by a similar-sized rainstorm event in the Orange County/San Diego region. As described in the following section, this difference leads to a consideration of watershed features as a principal factor influencing the relationship and correlation between stormwater and plume dynamics.

Watershed characteristics influencing the “rain/plume” relationship

The land-use properties of the drainage area where the discharge is formed appeared to be a pri-

mary factor regulating the quantitative relationship between stormwater and plume dynamics. The size of watershed area and its terrain also influenced this relationship. We realize that proper comparison between the watersheds in terms of their hydrology should be done using hydrological models of freshwater discharge, which take into account the detailed description of watershed physiography and land use. The amount of discharged water and pollutants from different areas of Southern California has been modeled using the Hydrologic Simulation Program-Fortran (HSPF; Ackerman and Schiff 2003, Ackerman *et al.* 2005). Modeling results illustrate that each km² of highly urbanized watershed contributes about twice the volume of total discharge than less urbanized areas (Ackerman and Schiff 2003). In this current study, we used a less formal approach, based on a qualitative comparison between the watersheds vis-à-vis their quantitative characteristics: the size of watershed area (Table 1), watershed terrain (Figure 10), and land-use properties (Figure 11). Also, the systems of hydrologic control (dams and reservoirs) are also taken into account. As a result, the general pattern observed (e.g., the differences between plume size, the slope coefficients in the linear rainfall/plume equations, etc.) is similar to the modeled results.

The size of the aggregated watershed area was not a primary factor regulating the typical size of the plumes observed in the nearshore coastal waters off Southern California. This result can be attributed to the fact that each of the four areas analyzed consisted of multiple watersheds, each with its own characteristics; thereby diminishing the effect of each individual watershed on plume size. However, when the difference between the aggregated watershed areas was dramatic, the rain/plume relationships were qualitatively different; e.g., in the smallest watershed of the SM region, the plume characteristics were different from the three other study regions. At the same time, when we compared the VE, SD, and SP regions, no direct correlation was revealed between the watershed area and the typical plume size. Largest plumes were observed in the VE region (Table 3; Figure 5), whose watersheds were not the largest; both the SP and SD watersheds exceeded Ventura in terms of area size (8762 - 9320 km² vs. 6831 km²). Previous studies (Mertes and Warrick 2001, Warrick and Fong 2004) of the quantitative relationship between the drainage (A) and river plume (P) areas indicated that these two parameters exhibited a power relationship ($P = c \times A^b$). We

explain this apparent contradiction by the fact that in this study we aggregated discharge estimates from multiple watersheds of different size, land use, hydrologic control, intrinsic sediment yield, etc., rather than individual watersheds with similar elevation and land-use characteristics. This aggregation likely confounded our ability to discern a clear relationship between watershed area and plume size.

According to our results, only in Santa Monica Bay did a smaller watershed area (1170 km²) result in much smaller plumes. In this region, only heavy rains (>2.5 cm) produced optical plume signatures comparable with the other three regions. Small and moderate rainstorms (<2.5 cm) contributed to detectable plume signatures, but this influence was much weaker than in other regions, resulting in a lower nLw555 estimated as the optimal plume boundary indicator. As such, freshwater plumes in Santa Monica Bay were qualitatively different from the plumes observed in the Ventura, San Pedro, and Orange County/San Diego regions. We attribute this difference to a combination of size, terrain and land use characteristics of the Santa Monica Bay catchment area, as well as watershed orientation and other intrinsic watershed properties. Specifically, Santa Monica Bay receives runoff from a broad range of land use types (developed vs. natural) that drain directly to the ocean via short, steep watersheds. In contrast, other watersheds are less heterogeneous and/or have larger areas to integrate different runoff sources.

The land-use characteristics of the watershed area influenced the interval between the rainstorm and the resulting plume. In the San Pedro region, where almost 40% of the drainage area was classified as “developed,” the period between a rainstorm and a plume maximum was one day, vs. two days for the three other regions. In Southern California, “developed” (industrial, commercial, and residential) areas are characterized by highly impervious surfaces, i.e., 40% - 85% impervious cover (Ackerman *et al.*, 2005), which have been shown to result in a greater proportion of precipitation translating to runoff in a shorter amount of time (Dunne and Leopold 1978). Similarly, the “runoff coefficient” (i.e., the runoff to rainfall volume ratio) in “developed” areas was estimated as 0.39 - 0.64 vs. 0.06 - 0.10 in “natural” areas, i.e., agricultural and open land (Ackerman and Schiff 2003). The effect of watershed impervious cover on runoff is amplified in the watersheds draining to the San Pedro shelf because most of the major rivers are lined with con-

crete, which further increases the magnitude and rate at which runoff reaches the coast (Gumprecht 1999). However, it is important to note that the upper portions of the Los Angeles and San Gabriel watersheds are controlled by a series of dams and basins which capture much of rainfall from the upper watershed and prevent it from reaching the coast, especially during smaller storms. These dams have the greatest effect on upper, more natural portions of the watersheds, with the lower, urbanized portions of the watersheds being subject to less hydrologic control. Therefore, the difference in effective land-use (i.e., the proportion of watershed land use not controlled by dams) between watersheds in the San Pedro region and other regions is even more dramatic. Based on effective land-use, impervious cover of the watersheds of Ventura and Orange County/San Diego regions is <10%. As a result, the relative amount of infiltrated water is higher and the time period of runoff flow to the ocean is longer. On the other hand, a slower flux of stormwater to the ocean resulted in more persistent plumes in Ventura and Orange County/San Diego areas ($k = 0.89 - 0.90$), as compared with San Pedro Shelf where $k = 0.75$. These coefficients indicate that, according to the primitive model we used in this study, in the San Pedro Shelf region 75% of stormwater was retained in the plume and 25% dissipated daily. In contrast, in the Ventura and Orange County/San Diego regions 90% of stormwater was retained in the plumes and only 10% dissipated. One explanation of this difference is a slower freshwater discharge, resulting in a slower response in terms of the optical signature in the coastal waters. Another explanation is the difference in coastal circulation. We hypothesize that in the shallow near-shore zone of the San Pedro Shelf, small-scale and mesoscale variability of ocean circulation was more intensive than in deeper Ventura and Orange County/San Diego regions (e.g., Hickey 1992 and DiGiacomo and Holt 2001), resulting in quicker plume erosion. The specific impact of these oceanographic features will be a focus of our future studies.

One interesting result was that the apparent nature of satellite-detected plumes in Santa Monica Bay was qualitatively different than in the other regions, as the optimal nLw555 backscattering coefficient serving as a local plume-indicator was substantially lower (0.8 mW cm⁻² μm⁻¹ sr⁻¹ vs. 1.3 mW cm⁻² μm⁻¹ sr⁻¹). Further, the time lag between rainstorms and plumes in the highly urbanized Santa Monica Bay watershed was two days, similar to

the less developed Ventura and Orange County/San Diego watersheds, but different, however, from the similarly urbanized San Pedro region, a seemingly anomalous result. In particular, comparing Santa Monica Bay to the San Pedro region, given their similarities in land use characteristics (~40-85% development of watersheds) we assumed that the stormwater precipitated over this small watershed should flow to the ocean immediately after the rainstorm as is the case in the San Pedro region (Ackerman and Weisberg 2003). However, the amount of stormwater accumulated over the Santa Monica Bay catchment area was relatively small overall, apparently impacting both the nature of the runoff (i.e., lower plume indicator value) as well as its timing, as discussed above. Another factor that distinguishes Santa Monica Bay from three other regions is its low elevation (Figure 10B) decreasing the speed of water runoff. The correlation between accumulated stormwater and plume area in Santa Monica Bay was not lower than in other regions, however, indicating rainstorms were still primarily responsible for the observed variability in the plume characteristics.

The terrain of each watershed also contributed to the relationship between rainfall and nearshore plumes. Ventura and Orange County/San Diego regions are similar in terms of watershed size and land-use characteristics. At the same time, in the Ventura watershed, 28% of drainage area is elevated >1000 m above sea level, vs. 15% in the Orange County/San Diego watershed at lower elevation. As a result, the plumes characteristic of the Ventura region were substantially larger than the plumes observed in Orange County/San Diego region. Another contributing factor is that in the Ventura region the bulk of freshwater discharge is concentrated from the Santa Clara River, in contrast to the Orange County/San Diego region, where stormwater is discharged to the ocean through several small rivers and creeks. Among other factors causing smaller plumes off the San Diego/Orange County coastline is the effect of numerous dams and bimodal watershed physiography, especially in San Diego County where river flow is often retained in the inland alluvial valleys. Also, the coastal plains in San Diego/Orange County have deep alluvial aquifers that are not completely paved, allowing more infiltration. Coastal wetlands (Newport Bay, Bolsa Chica, Batiquitos, San Dieguito, San Elijo, etc.) also may attenuate runoff and reduce plumes. The estimations of sediment

transport in different parts of the California coast (Mertes and Warrick 2001) reveal that small rivers contribute more sediment to the ocean near-shore zone than large rivers. However, the comparison here between the Ventura and Orange County/San Diego watersheds does not support this concept, indicating other factors (e.g., the terrain) can also influence the relationship between rainstorm magnitude and plume area size. Our results partly corroborate the conclusion of Milliman and Syvitski (1992) that maximum elevation of the river basin is a primary factor regulating sediment loads.

More extensive sediment plumes from the outlets of the Santa Clara and Ventura rivers likely result from higher concentration of sediments in its discharge, because these rivers drain the highly erosive western Transverse Range of California and are understood to be the largest sediment source of the SCB (Schwalbach and Gorsline 1985, Warrick *et al.* 2004b). Also, the mainstems of these rivers do not have any major dams to capture sediment. In contrast, most other Southern California watersheds have lower sediment yield and major dams that control sediment flow to the coast (e.g., Santa Ana River, San Gabriel River, San Diego River). Different sediment production probably affects the satellite signatures of the plumes.

Satellite signatures of plumes may be affected not only by the concentration of sediments, but also by sediment deposition in the nearshore zone, which acts to dilute the plume. Sediment deposition is mainly a function of the particle-size distribution within the plume and local and remote wind and tidal forcing. Ahn *et al.* (2005) studied particle size spectra in the Santa Ana River plume and showed that it progressively coarsened during the first few days after the rainstorm. They explain this observation as a result of within-plume coagulation of particles into larger size classes and, ultimately, removal of the largest particles by gravitational sedimentation. However, we have no data on the differences between the sediment size structures in different SCB regions; hence, this hypothesis needs future investigation. Furthermore, local hydrodynamic conditions can influence the rate of plume dilution. These issues will also be a focus of our future studies.

Different shapes of power regression equations (Figure 4; Table 3) also indicate the differences in land-use watershed characteristics as a primary factor influencing surface runoff. According to theoretical concepts developed by the Soil Conservation Service (Chow *et al.* 1988, Carlson 2004) the curve

$P_e = (P-0.2 \cdot S)^2 / (P+0.8 \cdot S)$ describing the relationship between the rainfall P and the excess (i.e., not infiltrated) precipitation P_e , which in turn forms the runoff, is linear when the land-use parameter S (called “potential maximum retention”) is zero. In highly developed impervious areas, S is very small; S increases in natural landscapes where the infiltration rate is higher. At higher S , the form of rainfall/runoff relationship becomes more curvilinear, which agrees with the results of our observations. The rainfall/plume (i.e., the rainfall/runoff) equation in the San Pedro region was almost linear, resulting from its physiography and land-use favoring an unimpeded discharge of rainfall to the ocean. In other regions, high infiltration rates in natural watersheds (Ventura and Orange County/San Diego), watersheds at low elevations (Santa Monica Bay region), and watershed physiography increased water retention, resulting in slower discharge of polluted surface water to coastal ocean.

LITERATURE CITED

- Acker, J.G., A.P. Vasilkov, D. Nadeau and N. Kuring. 2004. Use of SeaWiFS ocean color data to estimate neritic sediment mass transport from carbonate platforms for two hurricane-forced events. *Coral Reefs* 23:39-47.
- Acker, J.G., S. Shen, G. Leptoukh, G. Serafino, G. Feldman and C. McClain. 2002. SeaWiFS ocean color data archive and distribution system: assessment of system performance. *IEEE Transactions on Geoscience and Remote Sensing* 40:90-103.
- Ackerman, D. and S.B. Weisberg. 2003. Relationship between rainfall and beach bacterial concentrations on Santa Monica Bay beaches. *Journal of Water and Health* 1:85-89.
- Ackerman, D. and K. Schiff. 2003. Modeling storm water mass emissions to the Southern California Bight. *Journal of Environmental Engineering* 129:308-317.
- Ackerman, D., K.C. Schiff and S.B. Weisberg. 2005. Evaluating HSPF in an arid, urbanized watershed. *Journal of American Water Resources Association* 41:477-486.
- Ahn, J.H., S.B. Grant, C.Q. Surbeck, P.M. DiGiacomo, N.P. Nezlin and S. Jiang. 2005. Coastal water quality impact of stormwater runoff from an urban watershed in southern California. *Environmental Science and Technology* 39:5940-5953.
- Bailey, H.P. 1966. *The Climate of Southern California*. University of California Press. Berkeley, CA.
- Bay, S., B.H. Jones, K. Schiff and L. Washburn. 2003. Water quality impacts of stormwater discharges to Santa Monica Bay. *Marine Environmental Research* 56:205-223.
- Bertrand-Krajewski, J.-L., G. Chebbo and A. Saget. 1998. Distribution of pollutant mass vs volume in stormwater discharges and the first flush phenomenon. *Water Research* 32:2341-2356.
- Beuhler, M. 2003. Potential impacts of global warming on water resources in southern California. *Water Science and Technology* 47:165-168.
- Booth, D.B. 1990. Stream channel incision following drainage basin urbanization. *Water Resources Bulletin* 26:407-417.
- Cabelli, V.J., A.P. Dufour, L.J. McCabe and M.A. Levin. 1982. Swimming-associated gastroenteritis and water quality. *American Journal of Epidemiology* 115:606-616.
- Carlson, T.N. 2004. Analysis and prediction of surface runoff in an urbanizing watershed using satellite imagery. *Journal of the American Water Resources Association* 40:1087-1098.
- Chow, V.T., D.R. Maidment and L.W. Mays. 1988. *Applied Hydrology*. McGraw-Hill. New York, NY.
- Cristina, C.M. and J.J. Sansalone. 2003. "First flush," power law and particle separation diagrams for urban storm-water suspended particulates. *Journal of Environmental Engineering* 129:298-307.
- DiGiacomo, P.M. and B. Holt. 2001. Satellite observations of small coastal ocean eddies in the Southern California Bight. *Journal of Geophysical Research* 106:22521-22543.
- Dorman, C.E. and C.D. Winant. 1995. Buoy observations of the atmosphere along the west coast of the United States. *Journal of Geophysical Research* 100:16029-16044.

- Dunne, T. and L.B. Leopold. 1978. Water in Environmental Planning. W.H. Freeman. San Francisco, CA.
- Eganhouse, R.P. and M.I. Venkatesan. 1993. Chemical oceanography and geochemistry. pp. in M.D. Dailey, D.J. Reish, and J.W. Anderson (eds.), Ecology of the Southern California Bight. University of California Press. Berkeley, CA.
- Esaias, W.E., M.R. Abbott, I. Barton, O.B. Brown, J.W. Campbell, K.L. Carder, D.K. Clark, R.H. Evans, F.E. Hoge, H.R. Gordon, W.M. Balch, R.M. Leteller and P.J. Minnett. 1998. An overview of MODIS capabilities for ocean science observations. *IEEE Transactions on Geoscience and Remote Sensing* 36:1250-1265.
- Gumprecht, B. 1999. The Los Angeles River. Its Life, Death, and Possible Rebirth. Johns Hopkins University Press. Baltimore, MD.
- Haile, R.J., J.S. Witte, M. Gold, R. Cressey, C. McGee, R.C. Millikan, A. Glasser, N. Harawa, C. Ervin, P. Harmon, J. Harper, J. Dermand, J. Alamillo, K. Barrett, M. Nides and G.-Y. Wang. 1999. The health effects of swimming in ocean water contaminated by storm drain runoff. *Epidemiology* 10:355-363.
- Hickey, B.M. 1992. Circulation over the Santa Monica-San Pedro basin and shelf. *Progress in Oceanography* 30:37-115.
- Kirk, J.T.O. 1994. Light and photosynthesis in aquatic ecosystems. Cambridge University Press. Cambridge, MA.
- Lu, R., R.P. Turco, K. Stolzenbach, S.K., Friedlander, C. Xiong, K. Schiff, L. Tiefenthaler and G. Wang. 2003. Dry deposition of airborne trace metals on the Los Angeles Basin and adjacent coastal waters. *Journal of Geophysical Research* 108:4074, doi:10.1029/2001JD001446.
- McClain, C.R., Feldman, G.C. and S.B. Hooker. 2004. An overview of the SeaWiFS project and strategies for producing a climate research quality global ocean bio-optical time series. *Deep-Sea Research II* 51:5-42.
- Mertes, L.A.K. and J.A. Warrick. 2001. Measuring flood output from 110 coastal watersheds in California with field measurements and SeaWiFS. *Geology* 29:659-662.
- Mertes, L.A.K., M. Hickman, B. Waltenberger, A.L. Bortman, E. Inlander, C. McKenzie and J. Dvorsky. 1998. Synoptic views of sediment plumes and coastal geography of the Santa Barbara Channel, California. *Hydrological Processes* 12:967-979.
- Miller, R.L. and B.A. McKee. 2004. Using MODIS Terra 250 m imagery to map concentrations of total suspended matter in coastal waters. *Remote Sensing of Environment* 93:259-266.
- Milliman, J.D. and J.P.M. Syvitski. 1992. Geomorphic/tectonic control of sediment discharge to the ocean: The importance of small mountainous rivers. *Journal of Geology* 100:525-544.
- Nezlin, N.P. and E.D. Stein. 2005. Spatial and temporal patterns of remotely-sensed and field-measured rainfall in southern California. *Remote Sensing of Environment* 96:228-245.
- Nezlin, N.P. and P.M. DiGiacomo. 2005. Satellite ocean color observations of stormwater runoff plumes along the San Pedro Shelf (southern California) during 1997 to 2003. *Continental Shelf Research* 25:1692-1711.
- Noble, R.T., S.B. Weisberg, M.K. Leecaster, C.D. McGee, J.H. Dorsey, P. Vainik and V. Orozco-Borbon. 2003. Storm effects on regional beach water quality along the southern California shoreline. *Journal of Water and Health* 1:23-31.
- Otero, M.P. 2002. Spatial and temporal characteristics of sediment plumes and phytoplankton blooms in the Santa Barbara Channel. MS Thesis, University of California, Santa Barbara. Santa Barbara, CA.
- Otero, M.P. and D.A. Siegel. 2004. Spatial and temporal characteristics of sediment plumes and phytoplankton blooms in the Santa Barbara Channel. *Deep-Sea Research II* 51:1129-1149.
- Reeves, R.L., S.B. Grant, R.D. Mrse, C.M. Copil Oancea, B.F. Sanders and A.B. Boehm. 2004. Scaling and management of fecal indicator bacteria in runoff from a coastal urban watershed in south-

ern California. *Environmental Science and Technology* 38:2637-2648.

Sathyendranath, S. (ed.). 2000. Remote Sensing of Ocean Colour in Coastal and Other Optically-Complex Waters. Vol. 3. Reports of the International Ocean-Colour Coordinating Group. International Ocean Color Coordinating Group. Dartmouth, Nova Scotia.

Schiff, K.C. and S. Bay. 2003. Impacts of stormwater discharges on the nearshore benthic environment of Santa Monica Bay. *Marine Environmental Research* 56:225-243.

Schiff, K.C., M.J. Allen, E.Y. Zeng and S.M. Bay. 2000a. Southern California. *Marine Pollution Bulletin* 41:76-93.

Schiff, K.C., M.J. Allen, E.Y. Zeng and S.M. Bay. 2000b. Southern California. pp. 385-404 in: C.R.C. Sheppard (ed.), *Seas at the millennium : an environmental evaluation*. Pergamon. Amsterdam, NL.

Schwabach, J.R. and D.S. Gorsline. 1985. Holocene sediment budgets for the basins of the California continental borderland. *Journal of Sedimentary Petrology* 55:829-842.

Shipe, R.F., U. Passow, M.A. Brzezinski, W.M. Graham, D.K. Pak, D.A. Siegel and A.L. Alldredge. 2002. Effects of the 1997-98 El Nino on seasonal variations in suspended and sinking particles in the Santa Barbara basin. *Progress in Oceanography* 54:105-127.

Steinberger, A. and E.D. Stein. 2004. Effluent discharges to the Southern California Bight from large municipal wastewater treatment facilities in 2001 and 2002. pp. 2-15 in: S.B. Weisberg and D. Elmore (eds.), *Southern California Coastal Water Research Project Biennial Report 2003-2004*. Westminster, CA.

Svejkovsky, J. and B. Jones. 2001. Satellite imagery detects coastal stormwater and sewage runoff. *EOS* 82:621-630.

Toole, D.A. and D.A. Siegel. 2001. Modes and mechanisms of ocean color variability in the Santa Barbara Channel. *Journal of Geophysical Research* 106:26985-27000.

United States Geological Service (USGS). 1996. GTOPO30. <http://edcdaac.usgs.gov/gtopo30/gtopo30.asp>

Warrick, J.A. and D.A. Fong. 2004. Dispersal scaling from the world's rivers. *Geophysical Research Letters* 31. doi:10.1029/2003GL019114.

Warrick, J.A., L.A.K. Mertes, D.A. Siegel and C. MacKenzie. 2004a. Estimating suspended sediment concentrations in turbid coastal waters of the Santa Barbara Channel with SeaWiFS. *International Journal of Remote Sensing* 25:1995-2002.

Warrick, J.A. L.A.K. Mertes, L. Washburn and D.A. Siegel. 2004b. A conceptual model for river water and sediment dispersal in the Santa Barbara Channel, California. *Continental Shelf Research* 24:2029-2043.

Washburn, L., B.H. Jones, A.W. Bratkovich, T.D. Dickey and M.-S. Chen. 1992. Mixing, dispersion, and resuspension in vicinity of ocean wastewater plume. *Journal of Hydraulic Engineering* 118:38-58.

ACKNOWLEDGEMENTS

The authors would like to thank the SeaWiFS Project (Code 970.2) and the Distributed Active Archive Center (Code 902) at the National Aeronautics and Space Administration (NASA) Goddard Space Flight Center for the production and distribution of the SeaWiFS data and images, respectively. These activities were sponsored by NASA's Mission to Planet Earth Program. We also thank the National Oceanic and Atmospheric Administration (NOAA) National Data Center Climate Data Online (NNDC/CDO) for the rain gauge-measured precipitation data. Critical remarks by two anonymous reviewers helped to improve this paper substantially. The Jet Propulsion Laboratory (JPL) effort was supported by NASA, through a contract with JPL, California Institute of Technology.